Supplementary Material

Analysis of turnover dynamics of the submembranous actin cortex

M Fritzsche, A Lewalle, T Duke
London Centre for Nanotechnology and Department of Physics and Astronomy, University College London, London, United Kingdom

K Kruse
Theoretical Physics, Saarland University, Saarbrücken, Germany

G Charras
London Centre for Nanotechnology and Department of Cell & Developmental Biology , University College London, London, United Kingdom

I. DIFFUSIVE RECOVERY DYNAMICS AND BACKGROUND CORRECTION

The total fluorescence in the cortex results from proteins bound to the actin cortex and from proteins freely diffusing through the actin mesh. Therefore, after photobleaching, fluorescence recovery will have both a diffusive component and a reactive component resulting from proteins binding to and unbinding from the cortex. For a quantitative analysis of FRAP and FLAP data that goes beyond reporting half-times, the relative contributions of the two components need to be assessed. Depending on the relative kinetics of recovery of both contributions one can then make different approximations to develop a computational model, which is necessary for the data analysis [1].
To distinguish between the importance of the two components, we first determined fluorescence recovery of the purely diffusive protein GFP in the cytosol. GFP fluorescence was uniform in the cytoplasm and no accumulation or depletion of GFP in the cortical region could be detected. From this, we concluded that the cortical actin mesh did not present an obstacle to the diffusing GFP molecules and we performed FRAP experiments by bleaching a region in the cytoplasm. 50ms after bleaching, spatial heterogeneities were hardly detectable in the bleach region, Fig. S1A. Fluorescence recovery was fitted well by a single exponential function $\exp(-t/\tau)$ with a characteristic time $\tau \approx 50$ms, Fig. S1B.

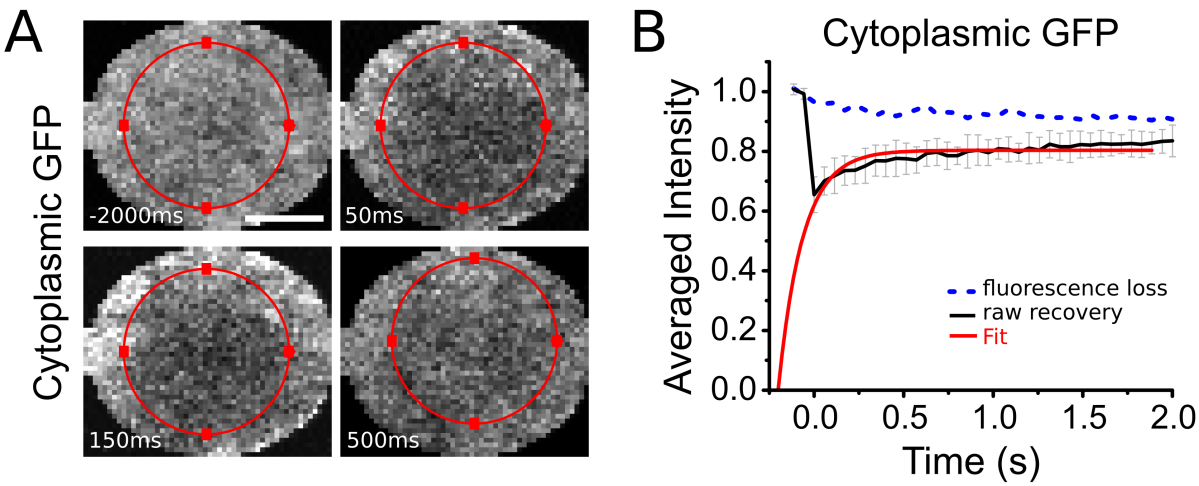

Figure S 1. Cytoplasmic GFP has a purely diffusive recovery. (A) Time series of a FRAP experiment in a cell expressing cytoplasmic GFP. The bleach zone is indicated by the red circle. Scale bar is 1μm. (B) GFP fluorescence recovery in the bleach region as a function of time. The red line is an exponential fit to the raw data (black line) with characteristic time $\tau \approx 50ms$. The blue line indicates fluorescence loss due to imaging.

The diffusion constants of G-actin, α-actinin, and myosin in the cytoplasm are similar to that of GFP and we assume the same to be true for these molecules in the cortex. We thus concluded that in our analysis we can neglect spatial aspects of the protein dynamics.
Furthermore, the above results show that recovery in the cytoplasm, which is essentially only due to diffusion, is much faster than in the cortex. Therefore it is safe to assume that the fluorescence resulting from free proteins in the cortical region of interest is the same as in the cytoplasm. To evaluate the amount of background fluorescence, we thus monitored fluorescence recovery in a region of cytoplasm contained within the bleach region away from the cortex, Fig. S2 and Fig. S3. To obtain the fluorescence signal from proteins bound to the cortex only (reactive component), we subtracted this background fluorescence (diffusive component) from the total fluorescence intensity in the cortical region of interest. In doing this, we also accounted for the differences in size of the cytoplasmic and the cortical regions of interest. For illustration, we show in Fig. S2 a fluorescence recovery curve for α-actinin and in Fig. S3 a fluorescence recovery curve for actin, with and without this background correction.

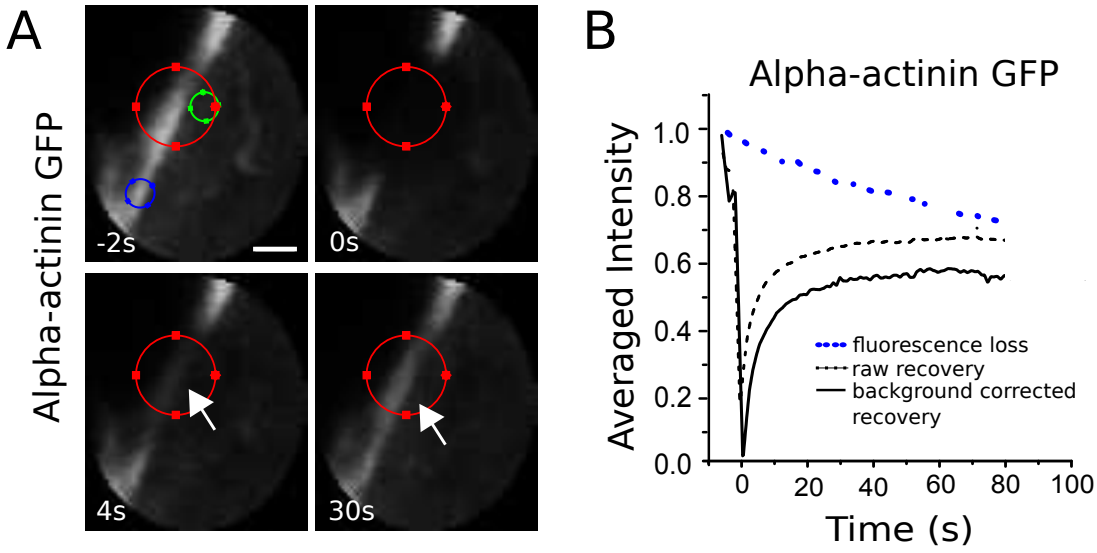

Figure S 2. Example of background correction for α-actinin-GFP FRAP. (A) Time series of a FRAP experiment in a cell expressing full-length α-actinin-GFP. The bleach zone is indicated by the red circle and was centered on the cortex (white arrow). Fluorescence from the background of freely diffusing proteins was estimated in a zone of cytoplasm included within the bleach zone (green circle). General loss of fluorescence due to imaging was monitored in a cortical region outside of the bleaching zone (blue circle). Scale-bar is 1μm. (B) Raw recovery of cortical fluorescence (black dashed line), cortical fluorescence recovery corrected for the contribution from the background of freely diffusing proteins (black line), and fluorescence loss due to imaging (blue dotted line) for the experiment in (A).

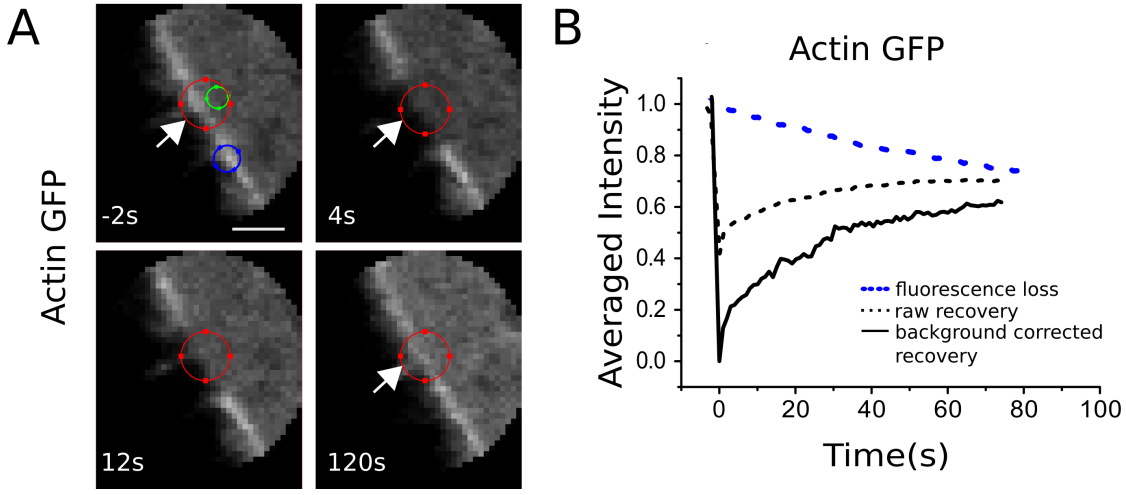

Figure S 3. Example of background correction for actin-GFP FRAP. (A) Time series of a FRAP experiment in a cell expressing actin-GFP. The bleach zone is indicated by the red circle and was centred on the cortex (white arrow). Fluorescence from the background of freely diffusing proteins was estimated in a zone of cytoplasm included within the bleach zone (green circle). General loss of fluorescence due to imaging was monitored in a cortical region outside of the bleaching zone (blue circle). Scale-bar is 1μm. (B) Raw recovery of cortical fluorescence (black dashed line), cortical fluorescence recovery corrected for the contribution from the background of freely diffusing proteins (black line), and fluorescence loss due to imaging (blue dotted line) for the experiment in (A).

II. FRAP DATA ANALYSIS BY FITTING MULTIPLE EXPONENTIALS

To analyse our fluorescence recovery data in the cortex, we fitted sums of exponential functions to each experimental curve. Specifically, we used $F(t) = \sum_{i=1}^{n} F_i(t)$ with

$$F_i(t) = \left(1 - \mathrm{e}^{-\omega_{\mathrm{d},i} t}\right) \frac{\omega_{\mathrm{a},i}}{\omega_{\mathrm{d},i}} F_0 + \mathrm{e}^{-\omega_{\mathrm{d},i} t} F_i(t=0), \tag{1}$$

see Eq. (2) in the main text. For each curve F_i, there are three fit parameters: $F_i(t=0)$, $\omega_{\mathrm{a},i} F_0$, and $\omega_{\mathrm{d},i}$. To determine the number n of exponentials, we first fitted one exponential, then two exponentials and so on until the following conditions were met: the goodness of fit estimated by the coefficient of determination r^2 no longer increased, the total change in fluorescence associated with process n was smaller than 10^{-5}, and the sum of squared errors no longer decreased. In Fig. S4, we give an example for this procedure for FRAP data obtained for α-Actinin-GFP, the corresponding fit parameters are summarized in Table I.

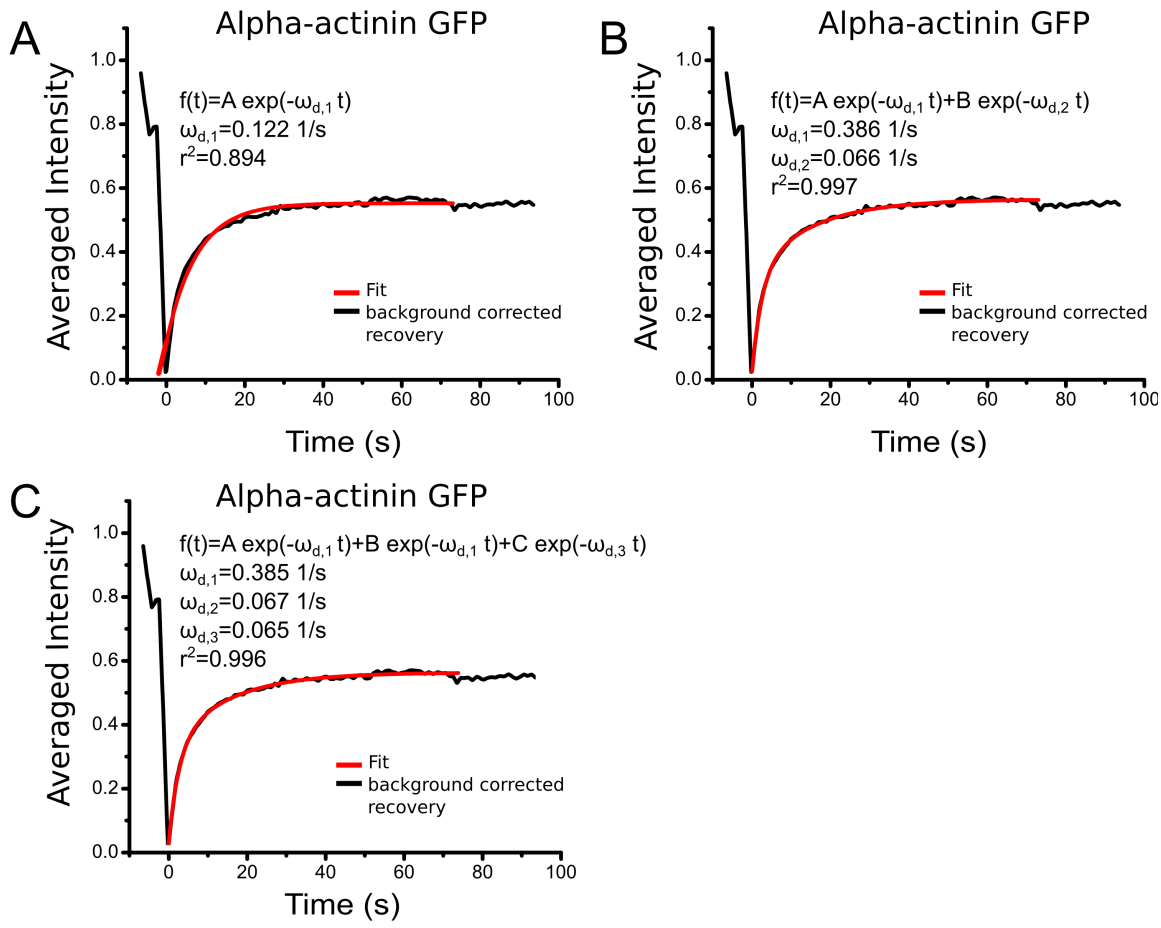

Figure S 4. Example of data analysis fitting increasing sums of exponentials to fluorescence recovery curves obtained from cells expressing full-length α-actinin-GFP. Fits with functions consisting of a single (A), two (B), and three (C) exponentials are shown. The fit function used as well as the goodness of fit are indicated on each panel.

n	$\omega_{d,1}$	$F_1(t=0)$	$\omega_{a,1}F_0$	$\omega_{d,2}$	$F_2(t=0)$	$\omega_{a,2}F_0$	$\omega_{d,3}$	$F_3(t=0)$	$\omega_{a,3}F_0$	r^2	χ^2
1	$0.122s^{-1}$	0	$0.06s^{-1}$	-	-	-	-	-	-	0.894	$2.4 \cdot 10^{-4}$
2	$0.386s^{-1}$	0	$0.01s^{-1}$	$0.066s^{-1}$	0	$0.02s^{-1}$	-	-	-	0.997	$2.8 \cdot 10^{-5}$
3	$0.385s^{-1}$	0	$0.01s^{-1}$	$0.067s^{-1}$	0	$0.01s^{-1}$	$0.065s^{-1}$	0	$0.01s^{-1}$	0.996	$3.8 \cdot 10^{-5}$

TABLE I. Fit parameters for exponential fits according to Eq. (1) and fit accuracy for different numbers of exponentials for the FRAP experiments on α-actinin in Fig. 4.

III. FRAP WITH FINER TIME RESOLUTION

In some of the experiments, we detected turnover processes with characteristic times $\tau = 1/\omega_d$ on the order of 1s, similar to the interval at which we sample fluorescence recovery. To verify that our sampling rate 1 frame per second (fps) yielded sufficient data points for the determination of the fast recovery rate, we repeated FRAP experiments using a higher sampling rate of 10fps. We here present the corresponding results for actin-GFP, which has the fastest recovery of the proteins we examined.

For a sampling rate of 10fps, we measured for 5s and fitted a single exponential to the data. We found an effective dissociation rate $\omega_{\mathrm{d},1}^{\mathrm{fast}} = 1.58 \pm 0.1\mathrm{s}^{-1}$ with $r^2 = 0.989$ ($N = 12$ cells), Fig. S5, comparable to that measured at lower sampling rates $\omega_{\mathrm{d},1} = 1.38 \pm 0.1\mathrm{s}^{-1}$ ($p = 0.9$ compared to $\omega_{\mathrm{d},1}^{\mathrm{fast}}$). No further improvement according to our criteria was obtained for $n = 2$ which yielded $\omega_{\mathrm{d},1} = 1.54 \pm 0.1\mathrm{s}^{-1}$, $\omega_{\mathrm{d},2} = 1.54 \pm 0.1\mathrm{s}^{-1}$ and $r^2 = 0.986$. We conclude that our results are robust against changes in the sampling rate. Sampling fluorescence recovery at 1fps allows for an accurate measurement of turnover rates and offers a good compromise between accuracy and minimisation of image-induced fluorescence loss.

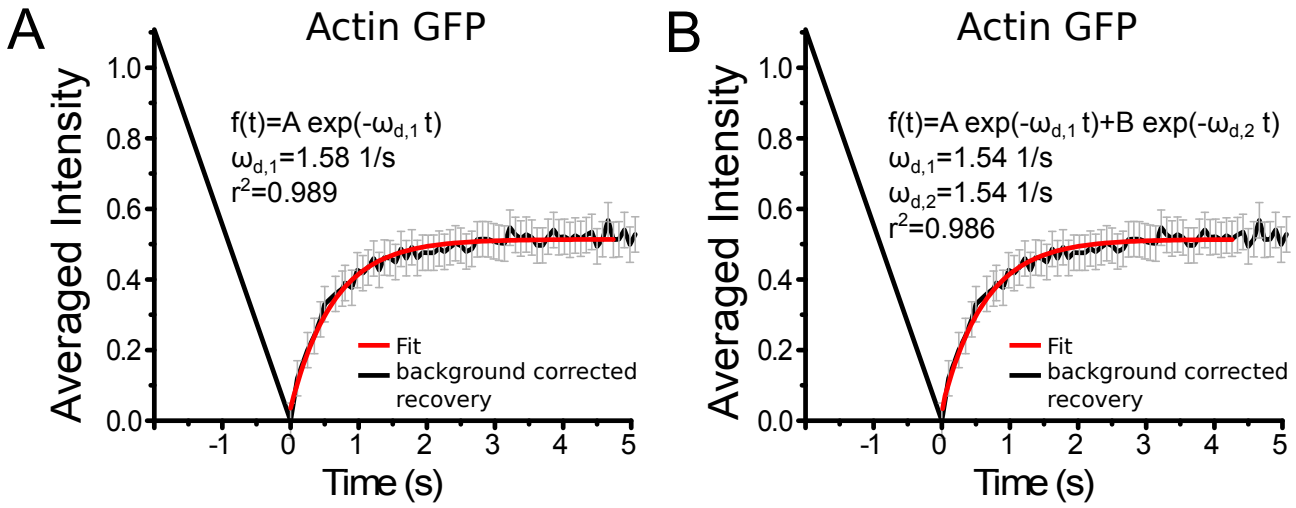

Figure S 5. Fluorescence recovery on short timescales in a cell expressing actin GFP. Fluorescence recovery acquired with a sampling rate of 10fps averaged over 12 cells. (A) Using one exponential, within errors, the corresponding effective dissociation rate $\omega_{\mathrm{d},1}^{\mathrm{fast}} = 1.58 \pm 0.1\mathrm{s}^{-1}$ with $r^2 = 0.989$ is very similar to the value obtained from experiments with a lower acquisition rate ($\omega_{\mathrm{d},1} = 1.38 \pm 0.1\mathrm{s}^{-1}$). (B) No further improvement according to our criteria was obtained for $n = 2$ yielding $\omega_{\mathrm{d},1} = 1.54 \pm 0.1\mathrm{s}^{-1}$, $\omega_{\mathrm{d},2} = 1.54 \pm 0.1\mathrm{s}^{-1}$ and $r^2 = 0.986$.

IV. LOGARITHMIC ACCELERATION PLOTS

The exponential dependence of fluorescence on time is best illustrated in logarithmic plots that present the logarithm of the fluorescence as a function of time. Indeed, if from a FLAP experiment, we get $F(t) = F_0 \exp(-\omega t)$, then $\log F(t) = \log F_0 - \omega t$, where F_0 is the initial fluorescence intensity and ω the fluorescence decay rate. From a FRAP experiment for a molecule with a single fluorescence recovery rate, we would get $F(t) = F_0(1 - \exp(-\omega t))$. Taking the derivative with respect to time, we get $dF(t)/dt = \omega F_0 \exp(-\omega t))$, that is an equation that is of the same form as

the equation for the fluorescence in FLAP. Again taking the logarithm one obtains a linear dependence as a function of time.
For visualization of the fluorescence data from FRAP/FLAP experiments, which contained several recovery/decay rates, it proved useful to plot the logarithm of the second derivative of the fluorescence signal with respect to time. Note that taking derivatives does not change the exponential dependence. Hence, to visualise the different processes participating in turnover as well as the effects of drug treatment and genetic perturbations on them, we produced plots of the logarithm of second derivative of F. We refer to them as logarithmic acceleration plots in the manuscript. They consist essentially of piecewise linear segments with each segment corresponding to a different process. The slopes of these segments are, respectively, $-\omega_{\mathrm{d},i}$. Changes in the recovery rates in response to drug treatment and genetic perturbations resulted in linear segments with steeper or shallower gradients that are easily visualised in the logarithmic acceleration plots.
‘

V. FRAP/FLAP INDUCED PHOTODAMAGE DOES NOT CAUSE SIGNIFICANT SEVERING OF ACTIN FILAMENTS IN THE CORTEX

As exposure to high local laser illumination may result in protein inactivation (a process known as chromophore assisted laser inactivation [2]), we asked if the subpopulation of actin filaments with fast turnover was due to the creation of free barbed ends by laser induced severing of actin filaments [3] using two independent experiments.

First, if photodamage induces severing of actin filaments and thus new barbed ends. Previous work has shown that local generation of free barbed ends by local uncaging of cofilin gives rise to a local increase in F-actin polymerisation [5]. Therefore, we reasoned that if photoactivation generated free barbed ends by laser-induced severing, we should observe an increase in the mRFP signal concomitant with photoactivation. To test if this occurs, we transfected cells with actin labelled with both mRFP and photoactivatable GFP (PAGFP-mRFP-actin, [4]) to allow for assessment of the turnover dynamics of photoactivated filaments with the PAGFP signal and imaging of total actin with the mRFP signal. Figure 6A shows consecutive confocal images of a cell expressing mRFP-PAGFP-actin in the red channel over the course of a FLAP experiment. The corresponding images for the green channel are shown in Fig. 2C in the main text. Photo-activation was performed in the region between the two red dots between times $t = 0$s and $t = 1$s. No local increase in mRFP-PAGFP-actin intensity denoting an increase in cortical F-actin density concomitant with photoactivation can be noticed. Panel B shows the temporal evolution of the fluorescence signal in the activation region (open circles, $N = 16$ cells) and this was not significantly different from the fluorescence loss due to imaging observed in a control region along the cortex outside of the activation region (black line, $N = 12$ cells). Furthermore, analysis of the fluorescence decay rate of the PAGFP signal allowed for independent determination of turnover. Two exponential functions were necessary to fit the PAGFP fluorescence decay curves with recovery rates $\omega_{\mathrm{d},1} = 1.1\pm0.2\mathrm{s}^{-1}$, $\omega_{\mathrm{d},2} = 0.04\pm0.01\mathrm{s}^{-1}$, $f_1 = 0.65\pm0.06$ ($N = 25$ out of 25 curves examined), Fig. 2D. The measured effective dissociation rates (recovery rates) obtained from the FRAP and FLAP experiments were not significantly different from one another ($p = 0.84$ and $p = 0.96$, for $\omega_{d,1}$ and $\omega_{d,2}$, respectively). As no severing occurred during FLAP, this implied that no severing occurred during FRAP either.
Second, as laser induced photodamage has been shown to be very sensitive to illumination settings [3], we varied the laser power used for photobleaching between 80% and 100% of maximal power reasoning that this should modulate the reaction rates and relative size of subpopulation 1 if it was due to laser-induced filament severing. Analysis of the fluorescence recovery revealed that neither the reaction rates nor the relative sizes of the two filament subpopulations were affected by changes in laser power, Fig. 6. The measured recovery rates of subpopulation 1 are summarized in Table II and the corresponding curves presented in Fig. 6C. For the three laser powers, the recovery rates were not significantly different from one another ($p \geq 0.9$).
Together, these data show that the subpopulation of actin filaments with fast turnover is not due to laser-induced filament severing.

laser power (% of maximum)	$\omega_{d,1}$	$\omega_{d,2}$	f_1	number of cells
80%	$1.23 \pm 0.2\mathrm{s}^{-1}$	$0.04 \pm 0.01\mathrm{s}^{-1}$	$f_1 = 0.66 \pm 0.1$	8
90%	$1.44 \pm 0.1\mathrm{s}^{-1}$	$0.04 \pm 0.01\mathrm{s}^{-1}$	$f_1 = 0.65 \pm 0.1$	16
100%	$1.38 \pm 0.1\mathrm{s}^{-1}$	$0.04 \pm 0.01\mathrm{s}^{-1}$	$f_1 = 0.65 \pm 0.06$	30

TABLE II. Measured turnover rates for various laser powers, Fig. 6C.

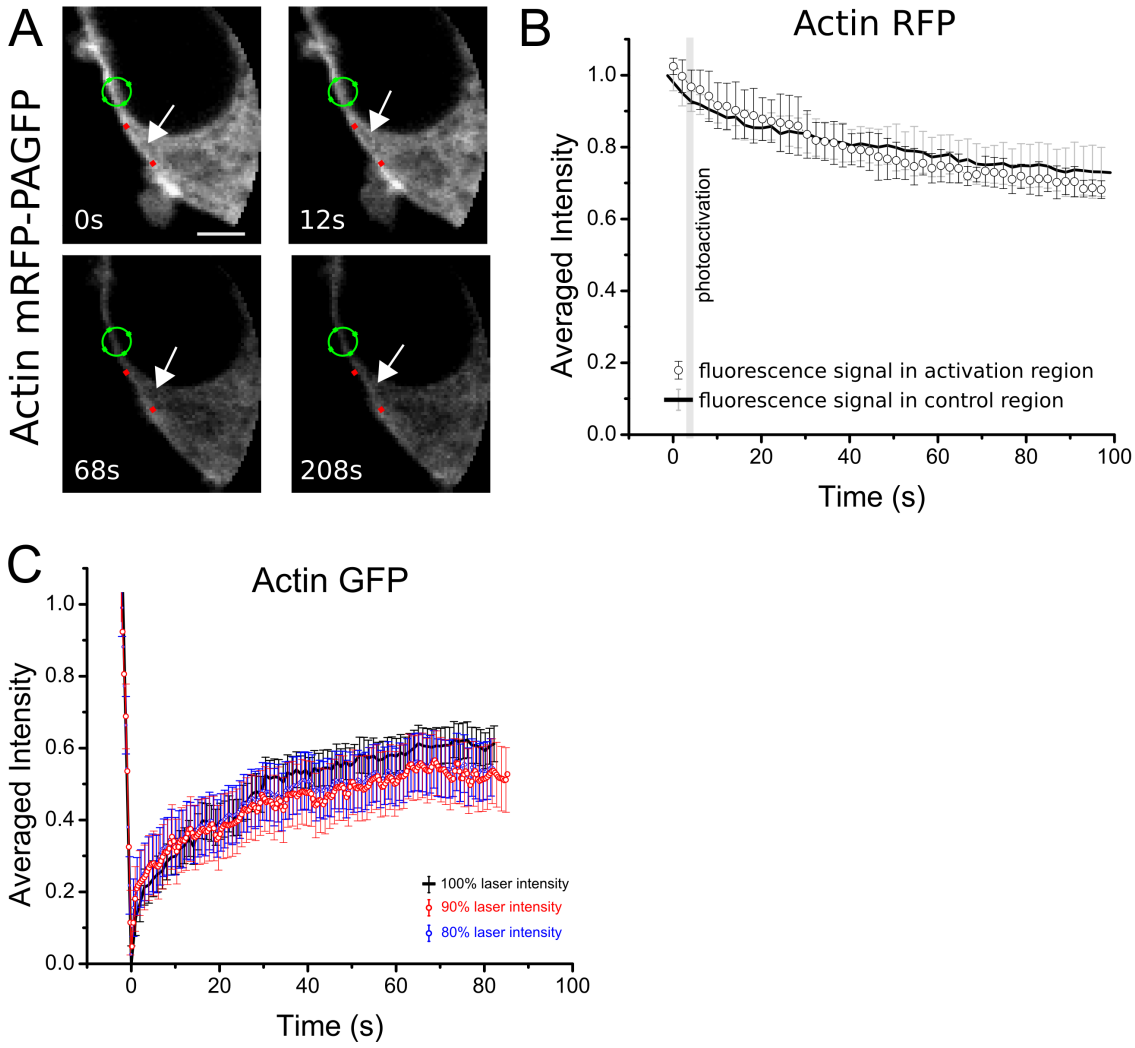

Figure S 6. The subpopulation of actin filaments with fast turnover is not due to laser-induced filament severing. (A) Time series of the mRFP fluorescence signal for a cell expressing mRFP-PAGFP-actin during a FLAP experiment. The fluorescence signal from PAGFP is shown in Figure 2C in the main text. Photo-activation was performed in between the two red dots between times $t = 0$s and $t = 1$s. The green circle indicates the location of a control region. The white arrow indicates the actin cortex in the region of photoactivation. Scale bar is 1μm. (B) Temporal evolution of the mRFP fluorescence signal in the activation region (open circles, averaged over $N = 16$ cells) and of the mRFP fluorescence loss curve (black line, $N = 12$ cells) in a control region close to the activation region (green region in A). (C) FRAP experiments in cells expressing GFP-actin for three different laser intensities: 80%, 90%, 100% of maximum laser output.

VI. PERTURBATION OF ACTIN CORTEX WITH CYTOCHALASIN D

After exposing Melanoma M2 cells to cytochalasin D (10μM), the total fluorescence intensity of the cortex decreased until it reached a plateau after about 30min, Fig. S7. The plateau extended up to 60min after drug addition and then fluorescence sharply decreased further until only isolated patches of fluorescent actin-GFP remained (white arrows, A). We considered the cells to be in a quasi-steady state between 30min and 60min after drug addition and did our FRAP experiments in this time window.

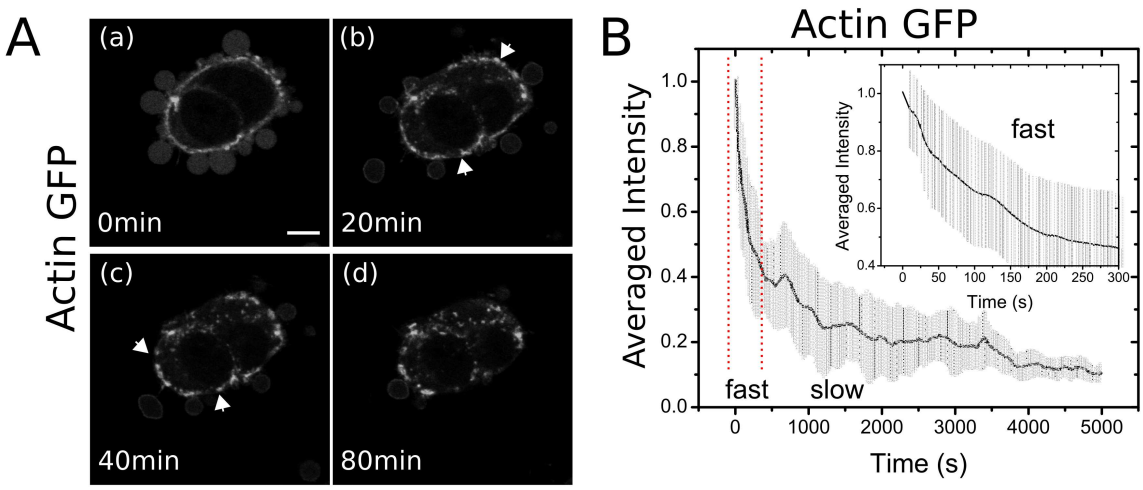

Figure S 7. Effect of cytochalasin D on the actin network. (A) Time series of confocal images of the cortex of cells expressing actin-GFP after addition of cytochalasin at $t = 0$min. (B) Total fluorescence intensity of cortical actin. Dotted lines indicate $t = 0$min and $t = 5$min. The curve is plotted as mean $\pm$ standard deviation for each time point. Inset: zoom on the first 300s of decay after cytochalasin treatment.

VII. PERTURBATION OF ACTIN CORTEX WITH LATRUNCULIN TREATMENT RESULTS IN PURELY DIFFUSIVE RECOVERY KINETICS

Latrunculin B treatment (520nM) resulted in complete disassembly of the actin cortex on a timescale of a few minutes. Figure S8A shows at 0s shows actin-GFP 15min after addition of Latrunculin B. A cortex is hardly visible. Photobleaching experiments show a purely diffusive recovery of actin-GFP, Fig. S8.

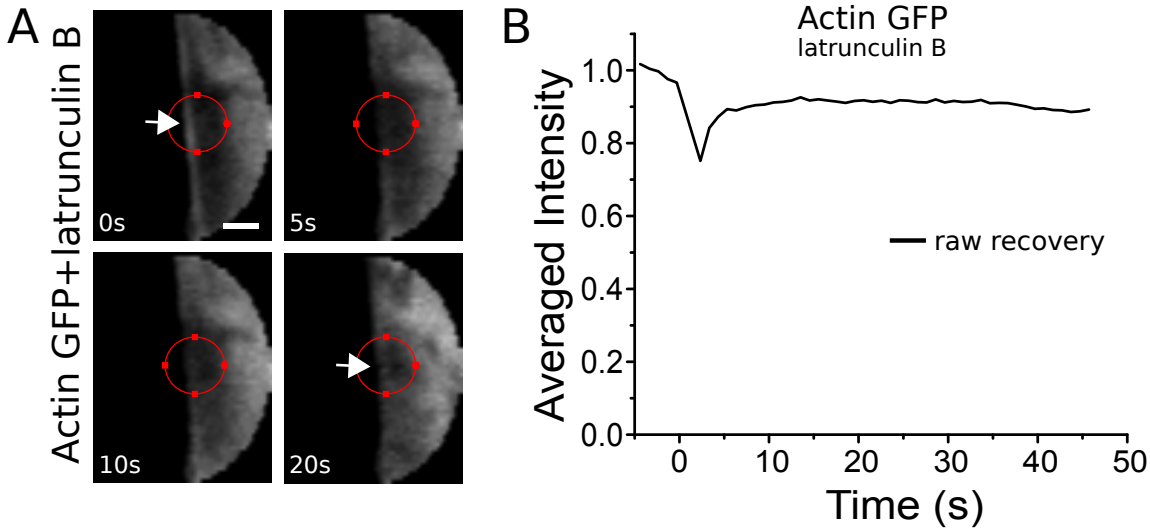

Figure S 8. Latrunculin B treatment of the actin cortex. (A) Time series of a FRAP experiment in a cell expressing actin tagged with GFP. The bleach zone is indicated with the red circle and was centered on the actin cortex (white arrow). Scale bar is 1μm. The actin cortex is fully disassembled 15min after latrunculin treatment. (B) Raw recovery of fluorescence (black dashed line) ($N = 25$ cells).

VIII. EXPRESSION OF DOMINANT COFILIN MUTANTS CHANGES THE F-ACTIN DENSITY IN THE CELL CORTEX

Melanoma M2 cells were fixed (Materials and Methods) and stained with FITC-phalloidin to measure the F-actin density in the cortex of control cells, in cells expressing constitutively active cofilinS3A, and in cells expressing constitutively inactive cofilinS3E, Fig. S9A. For presentation, the average cytoplasmic intensity was subtracted from the averaged cortical intensity, and finally normalised to the averaged cortical intensity in the control experiment, Fig. S9B. Our experiments shows that the total F-actin intensity decreases to $\sim 10\%$ of the initial F-actin mass in cells expressing constitutively active cofilinS3A ($p < 0.01$, $N = 18$ cells). In cells expressing constitutively inactive cofilinS3E, the total F-actin intensity almost doubled relative to control ($p < 0.01$, $N = 12$ cells).

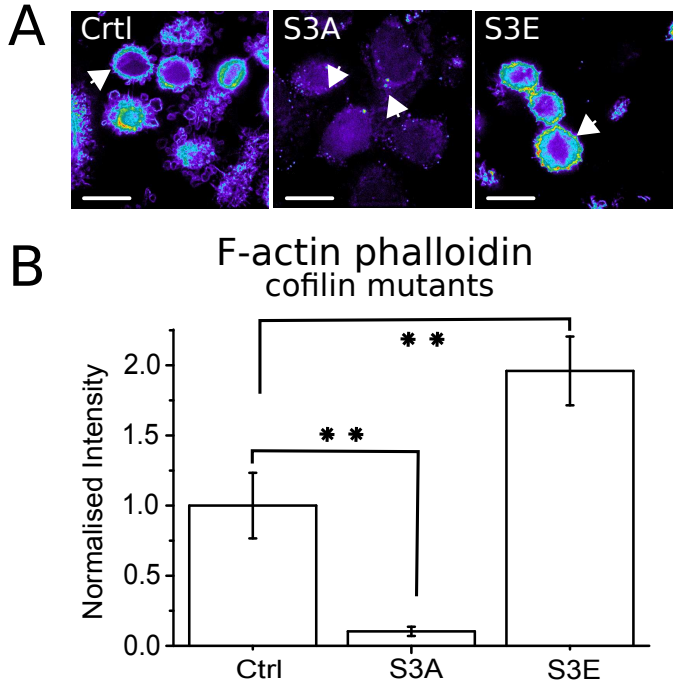

Figure S 9. Changes in F-actin mass in presence of cofilin mutants. (A) FITC-phalloidin fluorescence intensity in control cells, in cells expressing constitutively inactive cofilinS3E, and in cells expressing constitutively cofilinS3A. Fluorescence intensities are shown in false colors with warm colors reflecting high intensity and cold colors low intensity. Scale bar is 10μm. (B) Normalised fluorescence intensity for all three cases in (A).

IX. FRAP FOR THE ACTIN-BINDING DOMAIN OF α-ACTININ

In this section, we present our results on turnover of α-actinin's actin-binding domain tagged with GFP, Fig. S10. The actin-binding domain of α-actinin was predominantly localised to the cortex (Fig. S10B and movie S1). The recovery curve could be fitted well to a single exponential curve, Fig. S10C and Fig. 4 in the main text.

X. FRAP FOR MYOSIN REGULATORY LIGHT CHAIN (MRLC)

In this section, we present our results on turnover Myosin Regulatory Light Chain (MRLC). MRLC is a component of myosin II motors whose phosphorylation controls myosin activity. In FRAP experiments, MRLC recovery showed a half-time $t_{1/2} = 6.5\text{s}\pm1\text{s}$ ($N = 12$) and average effective detachment rate $\omega_d = 0.07\text{s}^{-1} \pm 0.04\text{s}^{-1}$, Fig. S11.

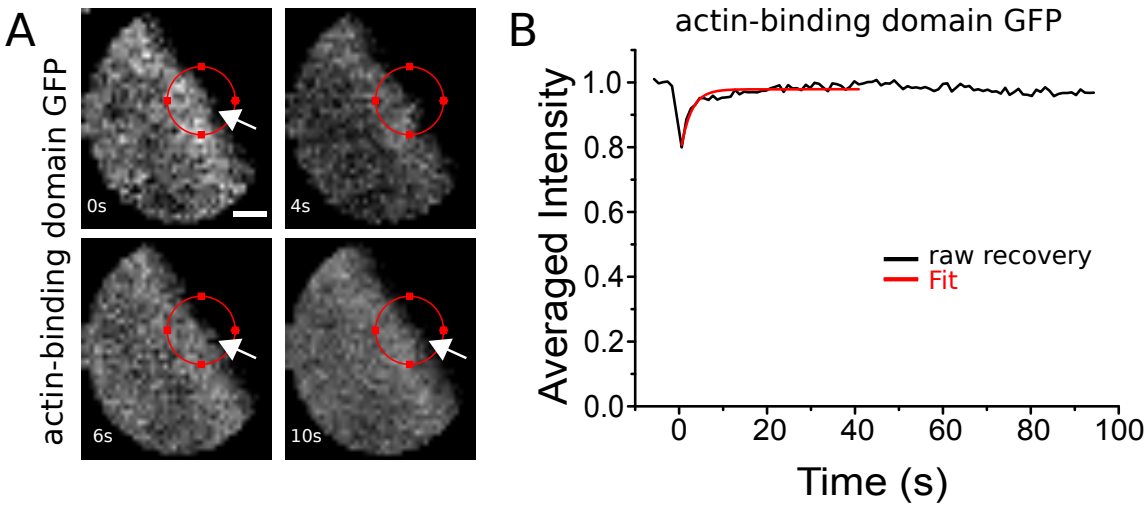

Figure S 10. (A) Time series of a FRAP experiment in a cell expressing the actin-binding domain of α-actinin tagged with GFP. The bleach zone is indicated by the red circle and was centered on the cortex (white arrow). Scale bar is 1μm. (B) Temporal evolution of fluorescence recovery. Actin-binding domain (black) shows a reactive recovery with a half-time of $t_{1/2}$ = 1s±1s ($N = 12$) and an effective dissociation rate of $\omega_d = 0.32 \pm 0.2\text{s}^{-1}$.

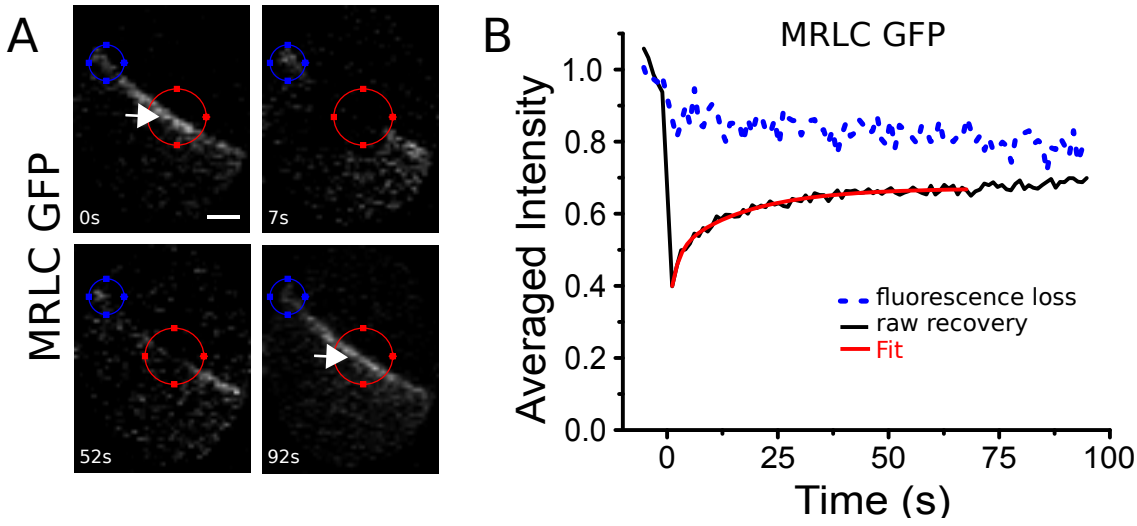

Figure S 11. (A) Time series of a FRAP experiment in a cell expressing MRLC tagged with GFP. The bleach zone is indicated by the red circle and was centered on the cortex (white arrow). General loss of fluorescence due to imaging was monitored in a region of cortex outside of the bleached zone (blue circle). Scale bar is 1 μm. (B) The cell cortex recovers with a half-time of $t_{1/2}$ = 6.5s±1s ($N = 12$ cells), and effective dissociation rates of $\omega_{d,1} = 0.6 \pm 0.1 s^{-1}$, and an $\omega_{d,2} = 0.07 \pm 0.04 s^{-1}$.

[1] Sprague B L, Pego R L, Stavreva D A, McNally G A (2004) Analysis of binding reactions by fluorescence recovery after photobleaching. Biophys J 86:3473–3495.
[2] Jacobson K, Rajfur Z, Vitriol E, Hahn K (2008) Chromophore-assisted laser inactivation in cell biology. Trends Cell Biol 18:443–450.
[3] Reymann A-C, Suarez, C, Guérin C, Martiel J-L, Staiger C J, Blanchoin L, and Boujemaa-Paterski R (2011) Turnover of branched actin filament networks by stochastic fragmentation with ADF/cofilin. Mol Biol Cell 22:2541–2550.
[4] Kueh H Y, Charras G T, Mitchison T J, Brieher W M (2008)Actin disassembly by cofilin, coronin, and Aip1 occurs in bursts and is inhibited by barbed-end cappers. J Cell Biol 182:341–353.

[5] Ghosh M, Song X, Mouneimne G, Sidani M, Lawrence D S, Condeelis J S (2004) Cofilin promotes actin polymerization and defines the direction of cell motility. Science 304:743–746.